TÜBİTAK

Turkish Journal of Earth Sciences

http://journals.tubitak.gov.tr/earth/

Research Article

Turkish J Earth Sci
(2015) 24: 56-71

doi:10.3906/yer-1403-7

Evidence of an active glacier in the Munzur Mountains, eastern Turkey

Cihan BAYRAKDAR[1,*], Zeynel ÇILĞIN[2], Mehmet Fatih DÖKER[3], Ergin CANPOLAT[2]

[1]Department of Geography, Faculty of Letters, İstanbul University, İstanbul, Turkey
[2]Division of Geography, Institute of Social Sciences, İstanbul University, İstanbul, Turkey
[3]Department of Geography, Faculty of Arts and Sciences, Sakarya University, Sakarya, Turkey

Received: 12.03.2014 • **Accepted:** 31.10.2014 • **Published Online:** 02.01.2015 • **Printed:** 30.01.2015

Abstract: The Munzur Mountains were subjected to extensive and repeated glaciations during the Pleistocene. The presence of an active glacier in the region was not verified until this study. Here, we used remote sensing methods to identify and locate the glaciers and verified the activity of the largest glacier in the field. We named this glacier the Şahintaşı Glacier and studied it using 3D ArcGIS spatial analyses overlaid on high-resolution Geographical Information Systems (GIS) satellite images. The most current version of LANDSAT 8 (acquired on 14.08.2013) supplied the remote sensing information. We used principal component analysis on the data. The precise areas where glaciers might be located were plotted. The data collection provided critical information to formulate an accurate representation of the Şahintaşı Glacier. The glacier dimensions are significant. It has a total area of 104,587 ± 10,458 m^2, with a length of 410 m, a width of 386 m, and an estimated maximum thickness of 90 ± 10 m. In the fore field, we identified 4 well-preserved terminal moraines. These moraines are remarkable in that the processes of their initial formation are immediately visible. The morphological properties of the cirque (its closure or high circularity, aspect, steepness, and near vertical walls), the high altitude, and the north-facing orientation are unique circumstances that have cumulatively helped preserve the Şahintaşı Glacier. The lithostratigraphic structure has had a large influence on the depth and circularity of the cirques. In the central section of the mountains, where the limestone is thicker, karstic development occurred vertically during the preglacial period, forming deep dolines that created steep-walled cirques and helped the glaciers survive until today. In addition, the mountains that are under the influence of northerly cold air masses in winter experience significant snowfall due to convective instability. The Munzur Mountains, which extend in an east-westerly direction in the manner of a 100-km wall and have summits surpassing 3000 m, allow for significant snow accumulation.

Key words: Munzur Mountains, Şahintaşı Glacier, Pleistocene glaciations, karst, glacial geomorphology, GIS and remote sensing

1. Introduction

Turkey is located in the Mediterranean climate zone. It has unique climatic and topographic diversities and influences due to its location; to geographic features, such as the Toros Mountains and Anatolian plateau; and to weather influences from the Black Sea and Mediterranean Sea. In Turkey, there is an abundance of mountains that exceed permanent snow lines, especially in the eastern Black Sea and eastern Anatolia regions, with many of these mountains encompassing active glaciers. The equilibrium line altitude (ELA) in the Quaternary glacier periods was between 2200 and 2400 m in the coastal regions and western Anatolia, and this threshold line significantly increases in the interior of the Anatolian plateau, with the lowest elevation at 3000 m and the highest at 3200 m (Figure 1). The present ELA and permanent snow lines on the north-facing slope (seaward slope) of the Rize Mountains and a section of the eastern Black Sea mountain range is 3100–3200 m. In the southern region of the country, the Taurus mountain range extends this line to 3400–3500 m. The wide range of the ELA is primarily due to continentality in the interior regions of Turkey; the ELA rises from west to east starting with an elevation of approximately 3500 m in central Turkey, 3700 m on Mount Süphan near Lake Van, and 4000 m on Mount Ararat (Erinç, 1952, 1971; Messerli, 1967; Atalay, 1987; Kurter and Sungur, 1991; Çiner, 2003; Akçar and Schlüchter, 2005; Sarıkaya et. al., 2011).

The glaciated areas in Turkey are in the high altitudes of the mountains, which extend in a line along the southeastern coast of the Black Sea (Erinç, 1945; Bilgin, 1969; Doğu et al., 1993; Akçar et.al., 2008; Gürgen and Yeşilyurt, 2012), the central and southeastern Taurus Mountains (Erinç, 1953; Klimchouk et al. 2006), and some stratovolcanoes, such as Erciyes (Erinç, 1951; Sarıkaya et.al., 2009) in central Turkey and Süphan and Ararat located in the far east of Turkey (Kurter and Sungur, 1991; Sarıkaya, 2012).

* Correspondence: cihanbyr@istanbul.edu.tr

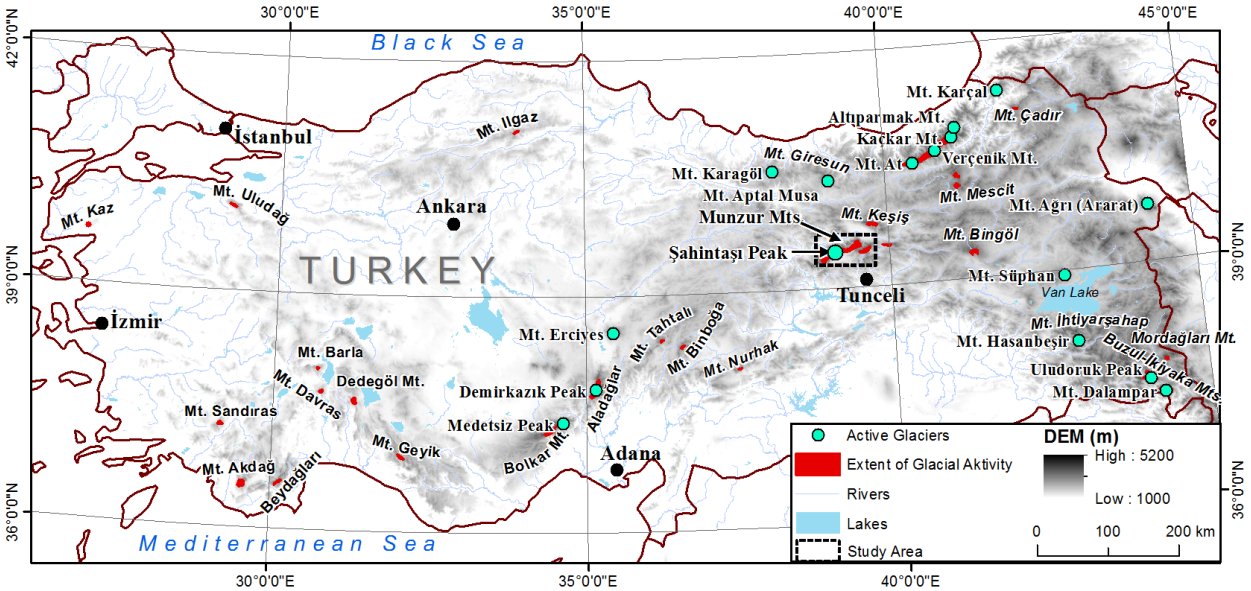

Figure 1. Active glaciers in Turkey and location of Munzur Mountains among the glaciated areas in Turkey.

The Munzur Mountains are located in eastern Anatolia between Erzincan and Tunceli Province (Figures 1 and 2). The Munzur mountain range exhibits erosional and depositional glacial landforms resulting from cold-period glaciations during the Pleistocene. In those times, the temperatures and climatic snow lines dropped due to a deteriorating weather trend. While the ELA is currently estimated between 3600 and 3700 m (Bilgin, 1972), it had actually descended to approximately 2750 m during the cold periods of the Pleistocene (Bilgin, 1972). The glaciations that occurred in the Munzur Mountains during the Pleistocene primarily came into existence in the form of mountain glaciations. In addition, small ice fields developed and were fed by the coalescing and merging of numerous cirque glaciers between summits that reached 3000 m and higher; these glacial zones would occasionally cover vast areas. These ice-field glaciers were fed by underlying cirque glaciers, and valley glaciers were cumulatively fed by all of the above. It is obvious from the glacier troughs, glacier tongue depressions, and moraines that the lobes of the valley glaciers descended to 1600 m and even lower to 1400 m, where the glacier trough ended in the Ovacık Plain (Bilgin, 1972; Çılğın, 2013).

Comprehensive research into the glacial geomorphology of the Munzur Mountains was conducted and the areas that were glaciated during the Pleistocene were mapped by Bilgin (1972). Supported by long-term field studies, he did not mention the presence of any active glaciers in his report.

Remote sensing work by Kurter and Sungur (1991) that encompassed the entire country of Turkey with the purpose of detecting glaciers did not reveal any active glaciers in the Munzur Mountains because the satellite images did not have high enough ground resolution. Subsequent work illustrating the distribution of active glaciers in Turkey (Çiner, 2003) did not mention or inventory any active glaciers in the Munzur Mountains. More recent studies based on remote sensing and utilizing satellite imagery with higher ground resolution (LANDSAT, Ikonos, Spot) indicated the presence of active glaciers in the Munzur Mountains (Yeşilyurt, 2010, 2012; Sarıkaya, 2011). Yeşilyurt (2010, 2012) claimed that there are more than 120 active glaciers in the Munzur Mountains and that these glaciers cover a 9-km^2 area, of which 1 km^2 is bare ice and 8 km^2 is covered by debris. In contrast with these results, Sarıkaya (2011) identified 13 cirque glaciers and 7 rock glaciers in the Munzur (Mercan) Mountains using Advanced Spaceborne Thermal Emission and Reflection Radiometer (ASTER) satellite images taken in August 2006.

These studies conclusively indicated the presence of glaciers, primarily due to the utilization of visible bands. However, the results were not supported or verified by a field survey in these studies. The importance of field verification is especially important due to the survival of yearly firn. Yearly firn can be erroneously identified as glaciers. However, the presence of glaciers has been well documented in mountains (Eastern Black Sea Mountains and Central Taurus Mountains) that have similar elevations to those of the Munzur Mountains. Still, even though the geographic settings and the geomorphologic and climatic characteristics of the Munzur Mountains are convenient for glaciation, it has not been possible to reveal the presence of glaciers in the mountains by checking in the field.

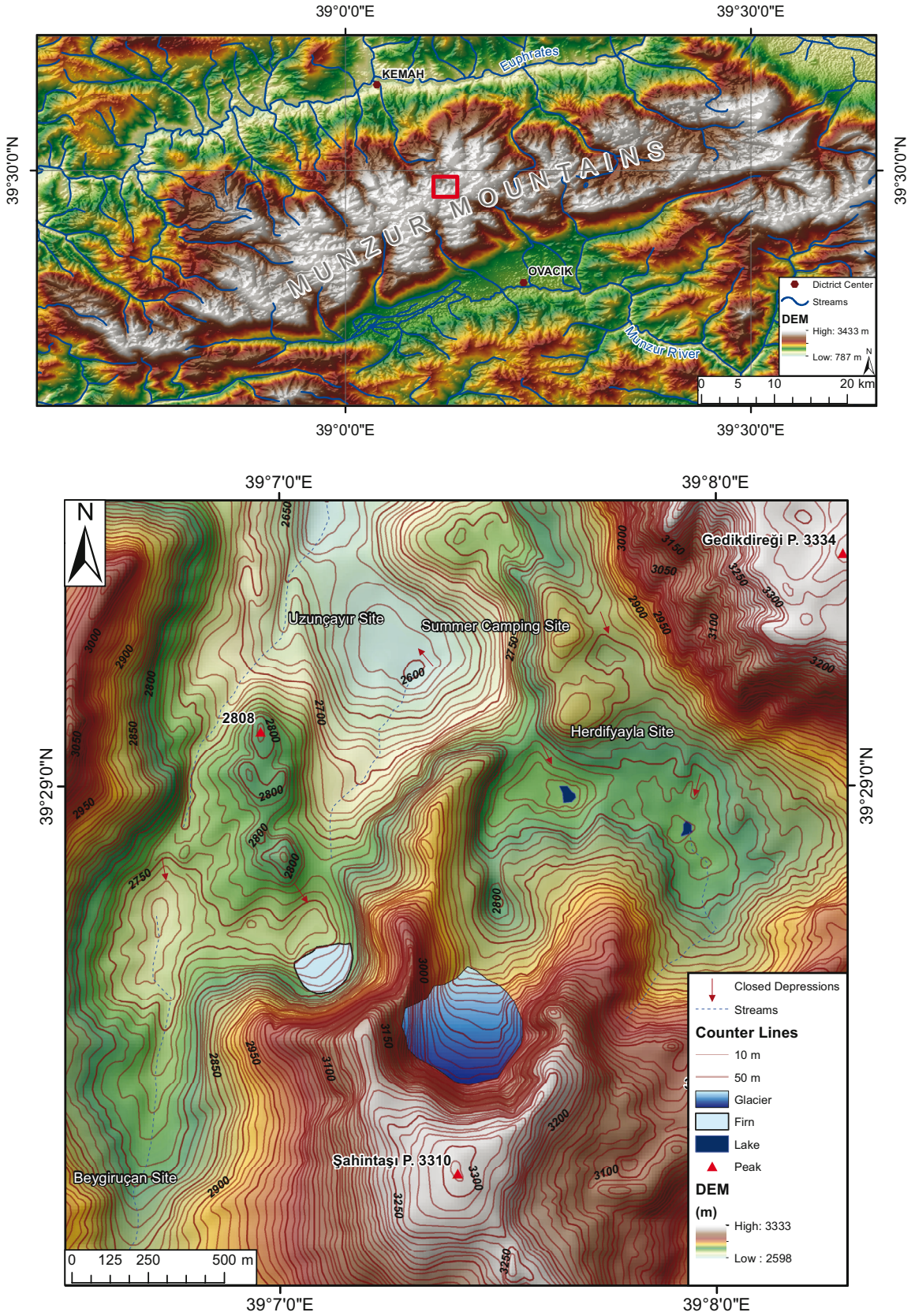

Figure 2. Location of the study area.

Through the use of satellite imaging (LANDSAT 8, August 2013), the application of principal component analysis (Sing and Harrison, 1985), and field work, this study discovered the Şahintaşı Glacier (adjacent to Şahintaşı Peak) in the Munzur Mountains, indicating the size, area, and thickness of the glacier. In accordance with the findings, the geomorphologic factors that have played a role in the preservation of this glacier have been explained.

The study area, comprising Şahintaşı Peak (3310 m) and its immediate surroundings, is located in the central part of the Munzur Mountains. This area presently houses one of the largest glaciers in the region. The glacier's name is derived from the nearby peak called Şahintaşı (Figure 3).

In 2013, the existence of an active glacier was verified by conducting a field survey whose goal was to map the area with an eye towards the glaciation processes that have occurred or are occurring there. In this respect, this was the first study of its kind to validate the presence of an active glacier on the Munzur Mountains by utilizing satellite imaging with thermal bands and then verifying the accuracy of the map by a survey in the field.

2. Method

Because glaciers are remote and require much effort to access, it is difficult to study and monitor them. Therefore, glaciologists and glacial geomorphologists rely on remote imaging to derive information about the characteristics of glaciers. Remote sensing images are defined as images taken above the earth's surface from either airborne platforms (e.g., cameras mounted on airplanes or helicopters) or spaceborne platforms (e.g., satellites). Hall and Martinec (1985), Jensen (1996), Lillesand and Kiefer (2000), and Rees (2001) gave further information on the physical principles of remote sensing, and Gao and Liu (2001) and Konig et al. (2001) provided recent reviews of the applications of remote sensing to glaciology and glacial geomorphology (Hubbard and Glasser, 2005).

Satellite imagery is valuable due to its ability to cover vast areas. At the same time, information about different characteristics of the earth's surface can be acquired using sensors that register different regions of the electromagnetic spectrum. The wavelengths frequently used in remote sensing are the visible range (0.4–0.7 μm), infrared (0.7–14 μm), and microwave (1–100 mm) (Lillesand et al., 2004). Multispectral optical sensors are used, such as ASTER and LANDSAT, to detect rays of the visible and infrared spectrum. Each spectral band is sensitive to a portion of the electromagnetic spectrum. Objects with a distinct material composition that have specific spectral reflections are rendered in a gray color tone to make these aspects of the terrain visible. In this respect, knowing the spectral reflections of the objects plays a significant role in selecting spectral bands.

Figure 3. Şahintaşı Glacier, view from the north (02.08.2013).

The data sources used in this study were gathered from 1:25,000 scaled topographical maps, 1:100,000 and 1:500,000 scaled geological maps, digital elevation maps created from counter lines with 10-m resolution, geographical positioning system (GPS) measurements, satellite imagery (2002 Geo Eye satellite images), and special maps resulting from field studies conducted in the summers of 2012 and 2013. The results were enhanced by means of high-resolution satellite images and using 3D spatial analyses. These data create a model and layering system that was integrated with a sophisticated database using Geographic Information Systems (GIS) software (ArcGIS 10.2) and remote sensing software (Erdas Imagine 9.1).

The study area was thoroughly researched using high-resolution satellite images (Google Earth) and LANDSAT satellite images that have higher spectral resolution, thus increasing the accuracy significantly. The LANDSAT 8 satellite data utilized in the study were downloaded from the US Geological Survey website (http://earthexplorer.usgs.gov/) with consideration for the time of year that had the least amount of snow cover. LANDSAT 8 started to receive images as of 20 May 2013.

The LANDSAT 8 Operational Land Imager and Thermal Infrared Sensor images consist of 9 spectral bands with a spatial resolution of 30 m for bands 1–7 and 9. New band 1 (ultrablue) is useful for coastal and aerosol studies. New band 9 is useful for cirrus cloud detection. The resolution for band 8 (panchromatic) is 15 m. Thermal bands 10 and 11 are useful for providing more accurate surface temperatures and are collected at 100 m (Table 1). Thus, we use only the 2–3–4 (visible bands), 5 (near infrared), and 6–7 (shortwave infrared) bands for this study.

LANDSAT 8 level 1 terrain-corrected (L1T) products are defined in the Universal Transverse Mercator map projection with the World Geodetic System 84 data and have improved geometric fidelity because of the LANDSAT

Table 1. LANDSAT 8 spectral designations (http://LANDSAT.usgs.gov/band_designations_LANDSAT_satellites.php).

	Bands	Wavelength (μm)	Resolution (m)	
LANDSAT 8 Operational Land Imager (OLI) and Thermal Infrared Sensor (TIRS) Launched 11 February 2013	Band 1 - Coastal aerosol	0.433–0.453	30	
	Band 2 - Blue	0.450–0.515	30	
	Band 3 - Green	0.525–0.600	30	Visible bands
	Band 4 - Red	0.630–0.680	30	
	Band 5 - Near Infrared (NIR)	0.845–0.885	30	NIR
	Band 6 - Shortwave Infrared (SWIR) 1	1.560–1.660	30	SWIR
	Band 7 - Shortwave Infrared (SWIR) 2	2.100–2.300	30	
	Band 8 - Panchromatic	0.500–0.680	15	Panchromatic
	Band 9 - Cirrus	1.360–1.390	30	
	Band 10 - Thermal Infrared (TIRS) 1	10.6–11.2	100	Thermal
	Band 11 - Thermal Infrared (TIRS) 2	11.5–12.5	100	

8 pushbroom sensor design and because the satellite has a fully operational onboard GPS, which can measure the exterior orientation directly rather than inferring it from ground control chips as with previous LANDSAT geolocation algorithms (Roy et al., 2014).

Taking into consideration the latest satellite images, the process of orthorectification is not necessary for this study because these images are simply used to indicate the presence of glaciers rather than for an accurate representation of their spatial features. At the same time, we have not carried out any atmospheric rectification on the downloaded LANDSAT images because there were no clouds, fog, or haze over the area harboring the glacier.

The LANDSAT satellite images were first layer-stacked in ERDAS Imagine software to obtain a multiple-banded image using the specific bands 2–3–4 (visible spectrum), 5 (near infrared), and 6–7 (shortwave infrared). The merged image was then subset to precisely define the outline of the study area (Figure 4).

The satellite data were first processed using an uncontrolled classification algorithm, based on classifying natural groupings and clusters in the image, to identify distinct features in the study area and to locate glaciers.

We used the Clustering-Iterative Self-Organizing Data Analysis Techniques (ISODATA) as an uncontrolled classification method. This helped acquire preliminary information about the study area. This process also had a negative result in that it caused difficulty in obtaining essential relevant information for the target area, such as discrepancies between the bands. An important step was added to compensate for these discrepancies. A significant image enhancement method called principal component analysis (PCA) was used to eliminate the discrepancies between multiple variables (multidimensional) (Figure 5). PCA compresses redundant data values into fewer bands, which are often more interpretable than the source data. It also helped suppress similar channels. This ultimately produced a new data set providing a much more accurate picture. Inclusion of most of the information was desirable and therefore the first 3 channels of the new data set produced through the PCA process were used (Jackson, 1983). PCA may also be used to compress the information content of a number of bands of imagery into just 2 or 3 transformed principal component images (Jensen, 1996). The bands of PCA data are noncorrelated and independent and are often more interpretable than the source data (Faust, 1989).

3. General geologic, geomorphologic, and climatic setting

The study area is situated in the central section of the Munzur Mountains, and the glacier is situated on the northwestern slope of Şahintaşı Peak (3310 m) (Figures 1 and 2). The Munzur Mountains have rugged alpine terrain. Thus, researchers have not been able to conduct research, especially on the glaciers, due to harsh topography, extreme weather conditions, scarce water supplies, and unfortunate security situations that intermittently close down the area.

The Munzur mountain range is located on the northeastern edge of the Taurus Orogenic Belt. The North Anatolian Fault dissects it. These mountains exhibit characteristics consistent with the larger geology, the Alpine Orogeny, which spans Turkey but also stretches from China to Europe. Munzur's limestone, which is primarily formed by shelf-type carbonates, represents a large part of the Mesozoic Era (upper Triassic-upper Cretaceous) (Özgül, 1981).

The Munzur Mountains are bordered by normal faults across the northern and southern slopes due to active tectonics, and they have wide and high erosional surfaces at or above 2800 m. A significant number of summits exceed

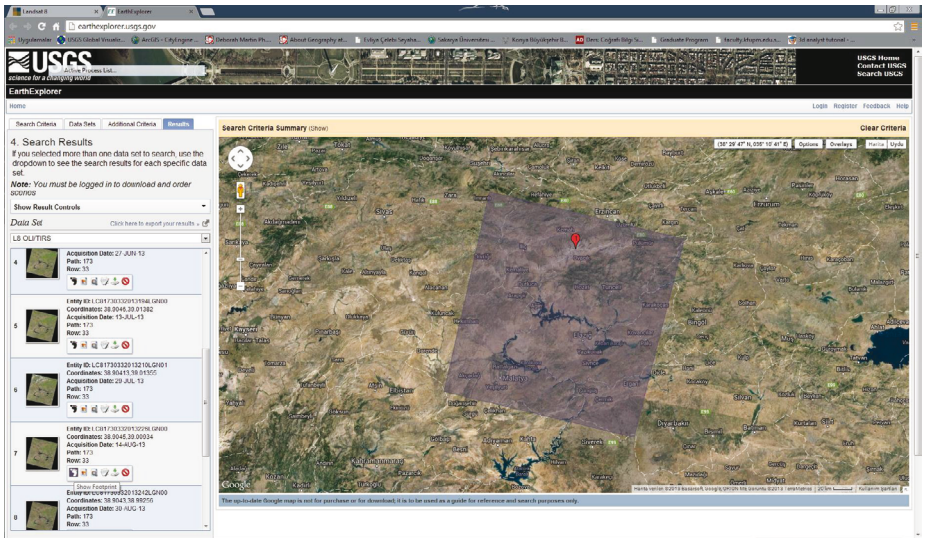

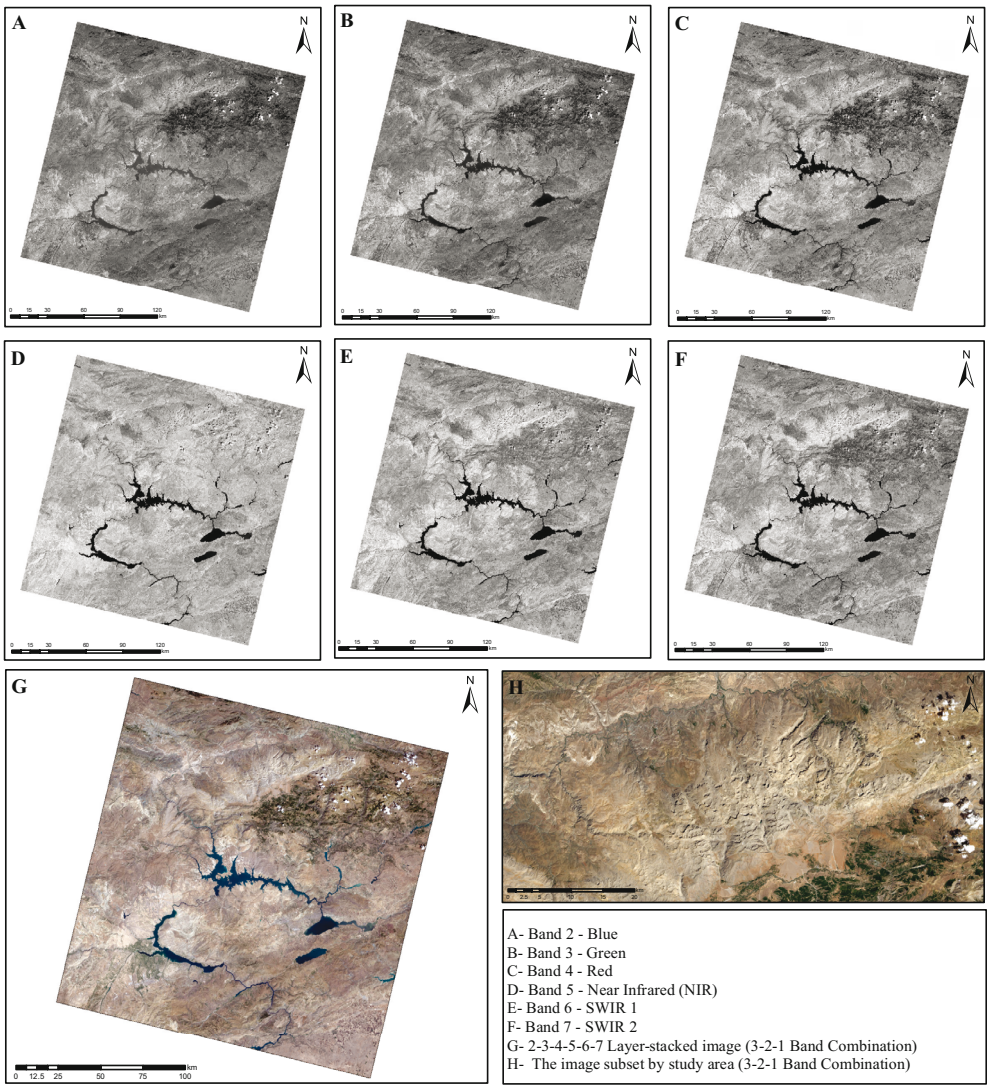

Figure 4. The Landsat 8 image of Munzur Mountains region (R–G–B: 3–2–1 band combinations).

3000 m on these erosional surfaces (Figure 2). The Munzur Mountains experience high humidity and moisture; thus, they are receptive to orographic precipitation due to massif characteristics being susceptible to climate changes during the Pleistocene. Because of these changes, the mountains have transformed the landscape through various factors and processes, resulting in polygenetic and polycyclic topography. Fluvial and karstic processes have played a key role in shaping the landscape, and this aggressive action continues today with subterranean drainages. Although glacial factors and processes have substantially diminished, their activity in the present and their contributions to the larger geomorphologic picture are significant, and the characteristics of this region are unique to this area of Turkey.

The general climate characteristics in the Munzur Mountains region have been classified using standards derived from the Turkish State Meteorological Service (www.dmi.gov.tr; Türkeş, 2010; Türkeş and Tatlı, 2011; Iyigun et al., 2013). According to the climate classification maps prepared by the Turkish State Meteorological Service and based on the methods of Thornthwaite, Erinç, and De Martonne, the Munzur Mountains region is classified as a subhumid climate. Precipitation constitutes the key reference point in these methods. The region is included in the humid continental climate type (D) according to Turkey's climate classifications, which evaluate both temperature and precipitation using the Köppen–Geiger method produced by Türkeş (2010). Worldwide, this climatic region represents a general humid zone with the average temperature of the warmest month below 10 °C and the average temperature of the coldest month reaching 0 °C or lower, characterizing the potential for extremely cold weather during some winters. The Munzur region can be further defined and classified as a climate with very cold winters and mild summers. According to the classification of precipitation regimes by Türkeş and Tatlı (2011), the study area is designated as a continental regime with primarily northerly weather system variables alongside convective instability occurrences and snow, which is quite dominant in winter. According to the most recent and detailed climate work (produced using 9 climatic variables), the Munzur Mountains region is classified as a subhumid continental zone in central-eastern Anatolia and a subregion that reflects a subhumid mesothermal and microthermal central and eastern Anatolian transitional climate (Iyigun et al., 2013).

Because there are no meteorological stations in the study area, we utilized meteorological data from nearby stations, such as Erzincan (1218 m) to the north, Tunceli (979 m) to the southwest, and Ovacık (1260 m) to the south. The meteorological data span the years of 1954–2013 for Erzincan and Tunceli (Table 2) and 1983–1991 for Ovacık. In light of these data, apart from small changes resulting from elevation and latitude, there are no significant temperature differences among the stations. However, there are significant differences in precipitation. While the annual precipitation of Erzincan is 373 mm, it is 868 mm for Tunceli (Table 2) and 1052 mm for Ovacık. Considering that mountains receive more precipitation than the lower areas around them, the precipitation rate in the Munzur Mountains must be higher than 1053 mm.

4. Şahintaşı Glacier – results

Şahintaşı Peak and the nearby area reflect typical traits of Pleistocene glaciation, and karstification occurred prior to this glaciation in the Munzur Mountains (Çılğın et al., 2014). While karst topography had been dominant in the area before the Pleistocene, glaciers covered vast areas through the consolidation of karstic depressions formed during glacial periods (Bayrakdar, 2012).

The cirques in the study area have generally developed on north-facing slopes. These cirques line up side to side and are separated by arêtes (Figure 6). The westernmost cirque has firn and developed along a N/NW direction (Figure 7). There is a terminal moraine in front of this cirque (Figure 8). The height on the median axis of the cirque is 440 m and the slope of the headwall is steep, nearing vertical (74°) (Figure 7).

The vertical distance between the glacier surface and the cirque crest is 240 m. The slope of the headwall is quite steep (71°) (Figure 7). The cirque had developed on the north-facing slope of Şahintaşı Peak (3310 m), which has characteristics of a pyramidal peak. The cirque walls exhibit consistent circularity with a width of 590 m and a length of 460 m.

The Şahintaşı Glacier extends on a sloping surface (approximately 20°) starting at an elevation of 2860 m and ending at 3020 m (from toe to head). The glacier has a total area of 10,4587 ± 10,458 m^2. Its maximum length and width are 410 m and 386 m, respectively. Ice on the floor of the cirque prevented us from getting a precise elevation measurement of the floor. For this reason, the exact thickness of the ice could not be determined. However, the morphometric features of a nearby cirque, which has firn, allowed us to indirectly extrapolate the altitude of this cirque's floor. Specifically, the visible headwall height of the cirque with firn is 440 m; the walls do not have high circularity and the cirque faces the NNW (Figures 7 and 8). There are cirque floors in the area that have a counter-slope behind the threshold. On the other hand, the traits of the Şahintaşı cirque, such as a higher headwall altitude, larger area, higher circularity, and northward orientation, all suggest that the cirque must be well developed in comparison to the cirque with firn. On such an occasion, the likelihood of cirque floors having a

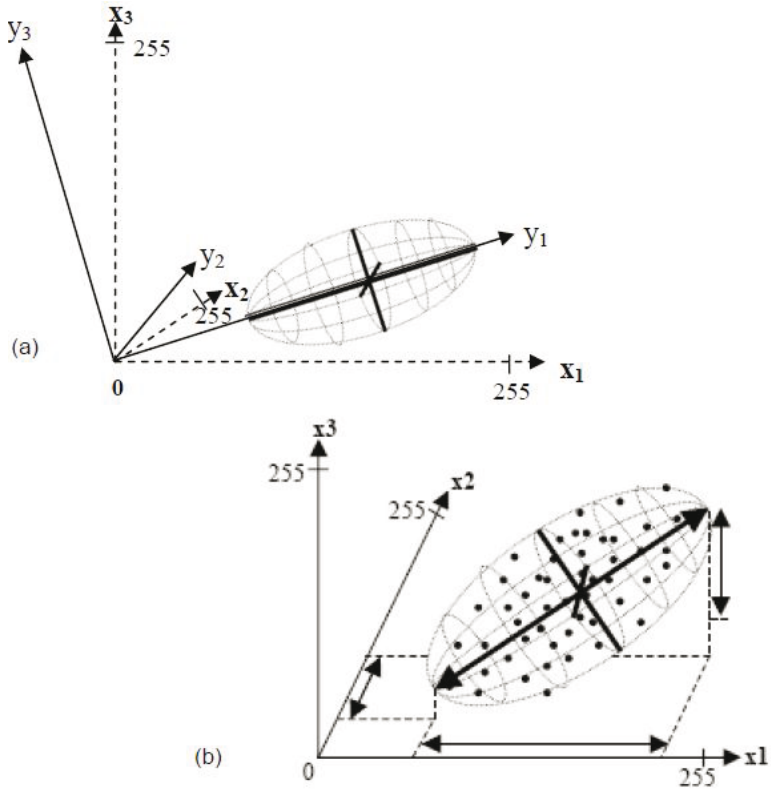

Figure 5. (a) Main component transformation. **(b)** Data representation range of first main component axis with regard to x1, x2, and x3 axes (Jackson, 1983).

counter-slope behind the threshold is quite high. Thus, the glacier modeling associated with this project estimates the ice thickness to be a maximum of 90 ± 10 m (Figure 6). This estimate and all of the other information rank this as the largest glacier in the Munzur mountain range.

Forbes bands (Paterson, 1994) are present in the Şahintaşı Glacier. Forbes bands, or ogives, form as glacier ice flows through an icefall area. Icefalls are causally related to the occurrence of very steep glacier beds. Here, the tensional stresses result in transverse crevassing and thinning while the ice moves through the fall. However, summer and winter conditions result in a modification of the ice as it moves through. Ice ablation during the summer results in thinner ice (and dirtier, because of dust collection) arriving at the foot of the fall. Precipitation during the winter, on the other hand, fills the crevasses with snow, resulting in thicker and cleaner ice arriving at the foot of the fall. For ice falls in which the ice moves through within a year's time span, the resulting situation at the foot of the fall, where the flow is compressive and crevasses are closed, are alternating ridges of blue ice (winter) and depressions of white ice (summer). These structures are convex in the direction of ice flow (even though the crevasses are slightly concave), indicating the differential motion in the transverse direction and in the longitudinal direction because of the crevassing (Sugden and John, 1976; Paterson, 1994; Hambrey, 1994).

These bands reflect different motion rates on the glacier surface and are slightly more convex where the ice motion is higher. Pieces of debris of various sizes that have fallen off the valley walls have covered the glacier surface. Very large boulders also appear in those materials (Figure 9).

There are 4 remarkable moraine ridges in front of the glacier. These are extraordinary in that they all have well-preserve initial forms (Figures 6 and 10). These moraines are proof and geomorphic evidence of receding periods for the glacier, indicating a warming trend from the last glacial period to the present day.

The first moraine ridge (I), which is the oldest of these 4 moraine ridges, is 460 m away from the glacier tongue, and its thickness is 45 m. This moraine ridge extends like a crescent shape, and there are several blocks on it, some of which are up to 4 m. The second moraine ridge (II) is 40 m behind the first and extends in a parallel manner with it. After these 2 moraine ridges, whose thicknesses are almost identical, the largest moraine ridge (III) appears 200 m away from the glaciers. The thickness of this moraine ridge is approximately 60 m and it has a slope of 30°. This moraine ridge elongates in front of the cirque from one end to the other. The last moraine ridge (IV) is situated

Table 2. Meteorological stations of Erzincan and Tunceli: long-term average values for 1954–2013 (Turkish State Meteorological Service, www.dmi.gov.tr).

	January		**February**		**March**		**April**		**May**		**June**		**July**		**August**		**September**		**October**		**November**		**December**	
Er / Tu	Er	Tu	Er	Tu	Er	Tu	Er	Tu	Er	Tu	Er	Tu	Er	Tu	Er	Tu	Er	Tu	Er	Tu	Er	Tu	Er	Tu
AT (°C)	–2.9	–1.9	–1.1	–0.4	4.4	5.6	10.8	12.0	15.6	17.1	20.0	22.7	24.0	27.3	23.8	26.8	18.9	21.6	12.1	14.6	5.2	7.0	0.0	1.0
AHT (°C)	1.7	2.7	3.7	4.5	9.7	10.9	16.7	17.9	22.1	23.8	27.0	29.9	31.4	34.9	31.8	35.1	27.3	30.4	20.0	22.6	11.5	13.4	4.5	5.4
ALT (°C)	–6.8	–5.8	–5.3	–4.5	–0.5	0.8	5.1	6.2	8.9	10.2	12.4	14.5	15.7	18.9	15.4	18.4	10.8	13.3	5.9	8.2	0.7	2.0	–3.6	–2.5
ASD (h)	3.6	3.2	3.6	4.1	5.1	5.3	5.5	6.3	7.4	8.5	9.6	11.2	11.0	11.6	10.2	11.1	8.6	9.4	6.3	6.5	4.3	5.0	2.4	3.0
ARD	9.7	11.9	9.5	12.0	11.8	12.8	13.9	13.7	14.4	12.3	9.1	5.1	3.2	1.5	2.4	1.1	4.4	2.7	8.4	8.3	8.8	9.6	10.0	11.6
MATP (kg/m^2)	27.6	125	31	111	40.6	112	53	110	53.7	71.0	29.7	18.8	11.0	3.2	6.2	2.6	14.4	13.7	40.2	64.0	37.1	105	28.3	132

Er: Erzincan (1218 m), 39°42′N, 39°31′E
Tu: Tunceli (979 m), 39°6′N, 39°32′E

AT: Average temperature (°C)
AHT: Average high temperature (°C)
ALT: Average low temperature (°C)
ASD: Average sunshine duration (h)
ARD: Average rainy days
MATP: Monthly average total precipitation (kg/m^2)

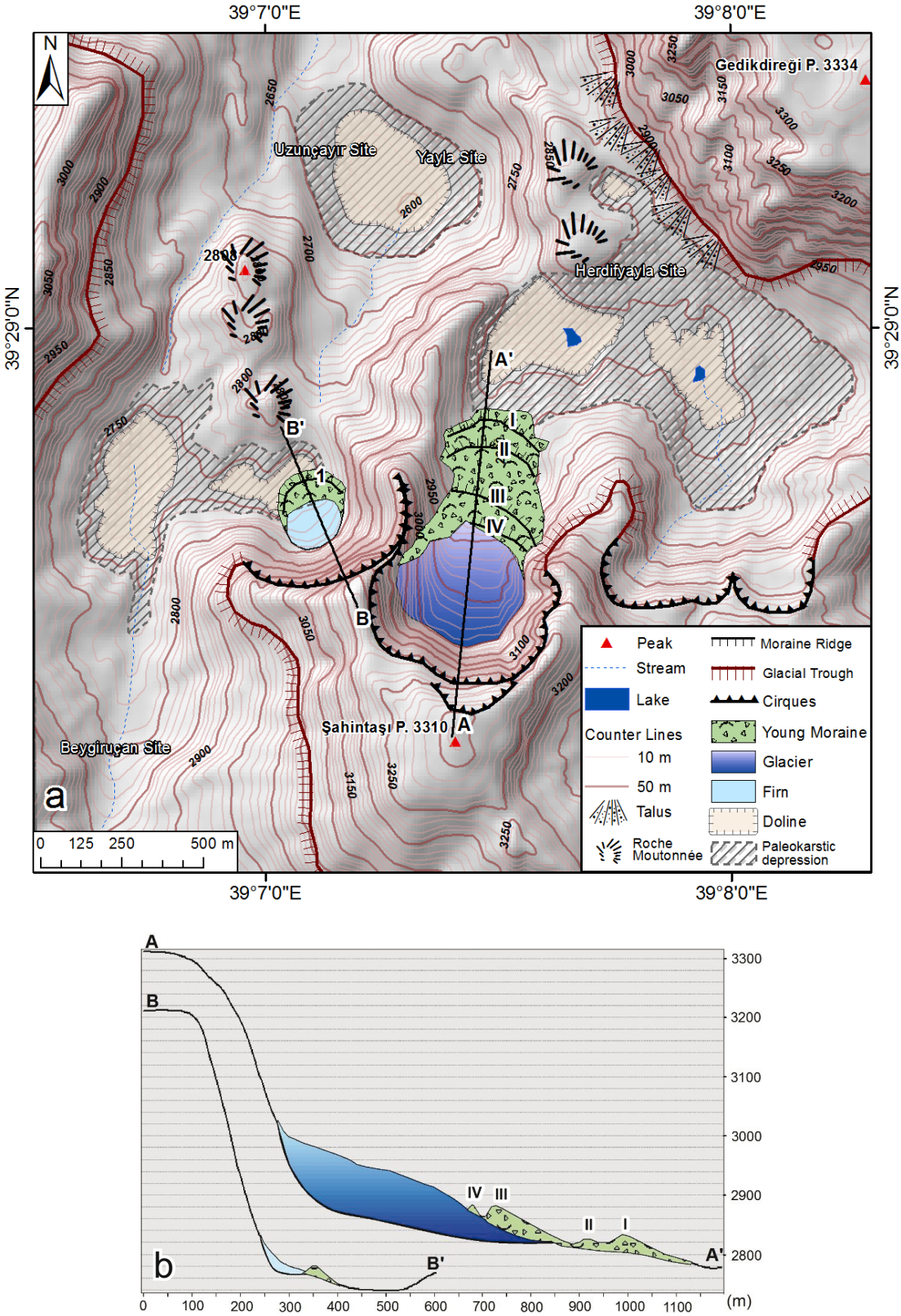

Figure 6. (a) Geomorphological map of Şahintaşı Glacier and its surroundings. **(b)** Longitudinal profiles of cirques (A-A' for the cirque with glacier and B-B' for the cirque with firn).

along the edge of the glacier tongue. Having a thickness of 20 m, this moraine ridge lies just to the east of the glacier tongue.

5. Discussion

The Munzur Mountains have immense summits surpassing 3000 m, but there are no glaciers on most of these summits. The largest glacier discovered in the mountains is the Şahintaşı Glacier.

The Şahintaşı Glacier was first detected through the use of high-resolution satellite data (Google Earth) containing visible bands. However, it is difficult to differentiate between permanent snow and glaciers in these images. Even detecting glaciers is problematic because most glaciers are covered with snow. For this reason, we used LANDSAT 8 data to detect glaciers because it has greater spectral resolution. When processing the data using an uncontrolled classification (ISODATA), we noticed that snow- and glacier-covered areas were mixed with each other. To solve this problem, a significant image enhancement method called PCA was used.

The PCA method, which was used to eliminate discrepancies between multiple variables (multidimensional), produce a new data set, and compress similar channels, yielded satisfactory results as it accurately detected glaciers. We assessed the method for distinguishing snow and glaciers in the field. As a result, the method has been verified (Figure 11).

The Şahintaşı Glacier is the largest active glacier in the Munzur mountain range. This glacier developed from the process of ice-field glaciation occurring at elevations of 2400 m or higher. Setting aside the factor of elevation, the geomorphological features of the Şahintaşı Peak and its immediate surroundings have also played a significant role in helping the Şahintaşı Glacier to survive. When compared to other cirques in the Munzur Mountains that have glaciers, the cirque that developed on the northern slope of Şahintaşı Peak is more favorable to the formation and survival of glaciers due to its higher elevation, circularity, and depth.

Active glaciers are most often located in the central section of a mountain range. Apart from elevation, the circularity and depth of the cirque have been quite important in helping this particular glacier survive. The lithostratigraphic structure has a share in the depth and circularity of the cirques. Although the rock formation consists primarily of limestone with consistent ages and rock properties, the thickness varies from place to place. While epikarst developed in the eastern section of the mountains, where ophiolite rocks and impermeable units encircle the limestone, karstic development occurred vertically during the preglacial period in the central section of the mountains where the limestone is thicker, forming vertical cave systems and dolines that became cirques during glacial periods. Therefore, these cirques have higher headwalls and more circularity when compared to those located in the western section of the mountains (Figures 6 and 12).

Apart from lithostratigraphic factors, the glacier's orientation has also affected its ability to survive. The cirque located to the west of Şahintaşı Glacier has a N/NW orientation. Given its lower degree of circularity, this has caused this cirque to have increased exposure to solar radiation, which prevented the glacier from surviving today. However, the elevation and height of the cirque and the steepness of the headwall all promote and support the formation of firn (Figure 13).

Two other connected cirques located in the eastern part of the study area reside at a lower elevation (3050 m). They have less wall height, circularity, and slope. Therefore, firn or glaciers have not been able to survive in these particular cirques.

Climatic and geomorphologic factors have significant bearing upon the presence of glaciers in the Munzur Mountains. Extending 100 km in an east-west direction and with high summits surpassing 3000 m, the Munzur Mountains allow for humid air masses from the Black Sea and Mediterranean Sea to build and meet. Because of this characteristic, the Munzur Mountains have more precipitation than the mountains surrounding them. The precipitation is predominantly snow throughout the year, which has promoted the growth of glaciers due to the high elevation of the mountains.

When examining the annual precipitation of the Ovacık and Tunceli stations, both stations receive a good amount of precipitation, especially in the winter, which is associated with southwesterly air masses from Mediterranean frontal systems.

It has been indicated by previous studies that a significant amount of snow falls due to the convective instability of the air masses in the winter. Being a massive range, with an elevation of 3000 m and over, the Munzur Mountains are a prominent area supporting conditions that are favorable to significant snow accumulation.

We propose that the Şahintaşı Glacier is a remnant of the Last Glacial Maximum. However, this glacier might have formed in the Little Ice Age. The exact period in which this glacier formed can be revealed by dating the moraines in front of the glacier. In a continuation of this study, we aim to reveal the age of the glaciers through cosmogenic dating methods.

6. Conclusions

This study has 2 major focuses. The first is identifying the morphometric features of the Şahintaşı Glacier, the largest Pleistocene remnant glacier in the area. The second is

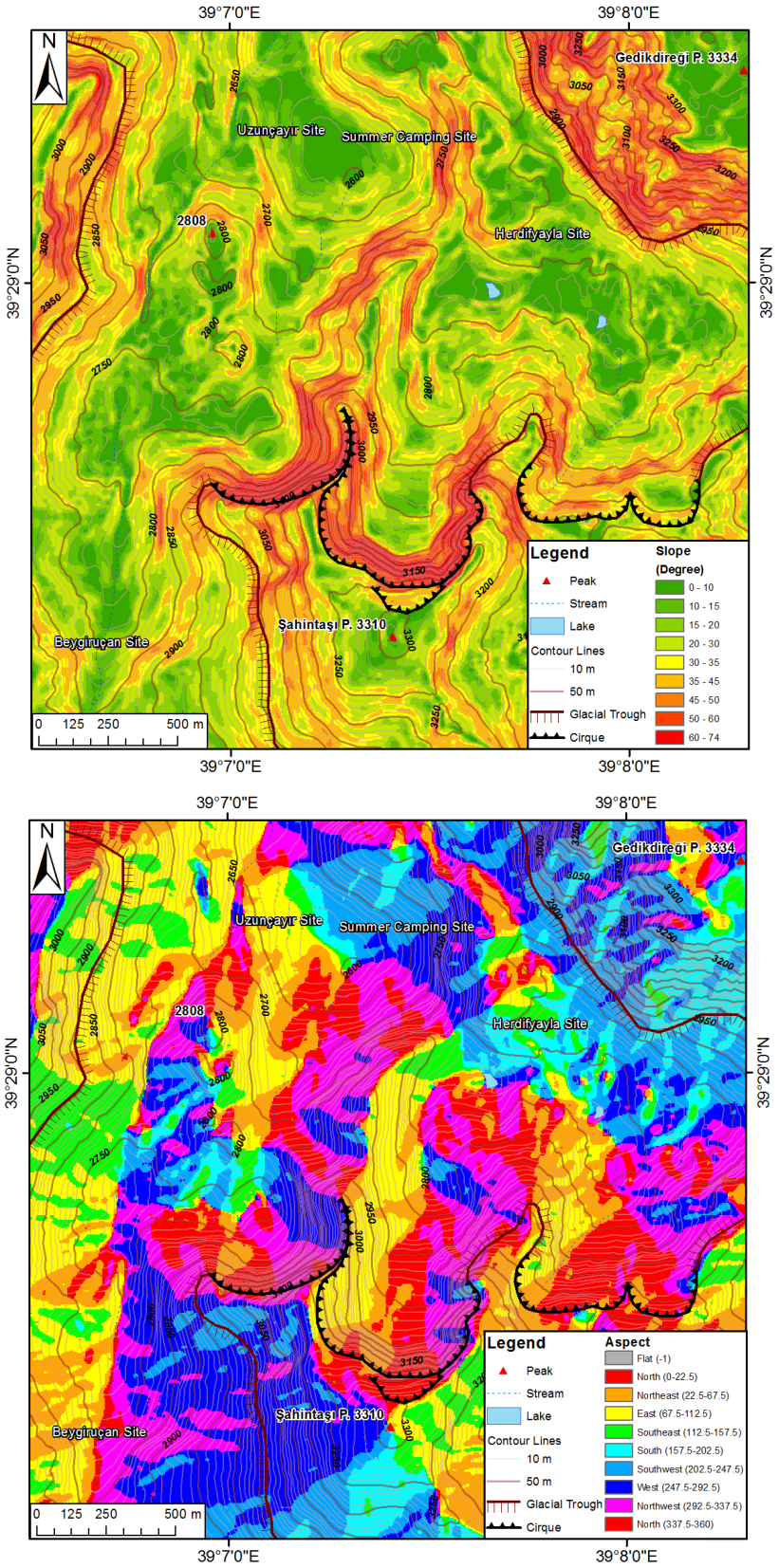

Figure 7. Slope (above) and aspect (below) properties of Şahintaşı Glacier and its surroundings.

Figure 8. Firn inside of the cirque with steep headwall toward the west of Şahintaşı Glacier and young terminal moraine in front of the cirque (view from northwest).

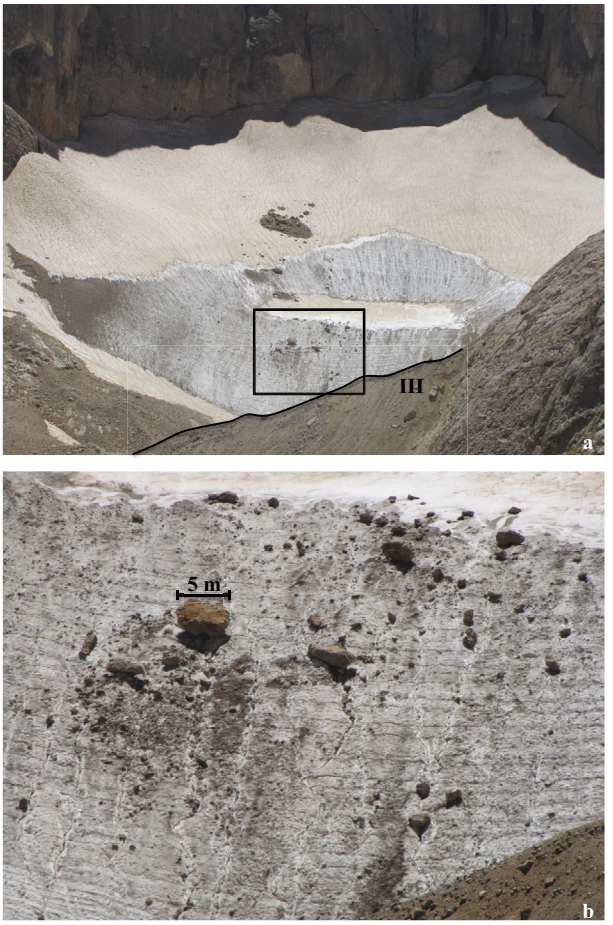

Figure 9. (a) Forbes bands on the glacier reflecting accumulations of different years and **(b)** a close view of the glacier (02.08.2013).

evaluating the geomorphological evolution of the adjacent area through satellite imagery and field surveys. This is the first study of its kind to identify and verify that a large, active glacier exists in the Munzur Mountains.

The presence of glaciers in the Munzur Mountains was first revealed by satellite images. We used LANDSAT 8 data to reveal glaciers. Using a satellite image of LANDSAT 8 by applying PCA, we acquired favorable results and made a clear distinction between glaciers and permanent snows.

During the Pleistocene, Turkey's alpine region, including the Munzur Mountains, was primarily covered by glaciers, and karstification intensity slowed or nearly stopped. Due to counteracting processes, the Şahintaşı Glacier and its immediate surroundings best represent classic polygenetic landform evolution. Glaciers have covered paleokarstic depressions in this area since the Pleistocene period, and some permanent ice coverage continues today in some areas. The remnants of the surviving glaciers have changed over time, receding and retreating in warmer periods.

Four recessional moraine ridges in front of the Şahintaşı Glacier indicate that the glacier has been in a retreating state. Despite changes over time, the glacier has survived up to the present. The morphological features (circularity, aspect, very steep headwall) and elevation of the cirque have been effective in helping the glacier survive. The glacier covers an area of 104,587 ± 10,458 m^2. Its maximum length and width is 410 m and 386 m, respectively. The maximum thickness of the ice has been estimated as 90 ± 10 m. These figures make the Şahintaşı Glacier the largest glacier in the region.

The geographical setting of the mountains is favorable, as its east-west extensional direction as a massive range of 3000 m has led the Munzur Mountains to be affected by northerly air systems. The convective instability of the air masses results in a significant amount of snowfall in the winter. Furthermore, conditions that promote long accumulations of snow have allowed the glacier to endure until today.

This is a preliminary study revealing the existence of an active glacier in the Munzur Mountains. Subsequent projects should be conducted to reveal the advancing and retreating periods of the glaciers through cosmogenic

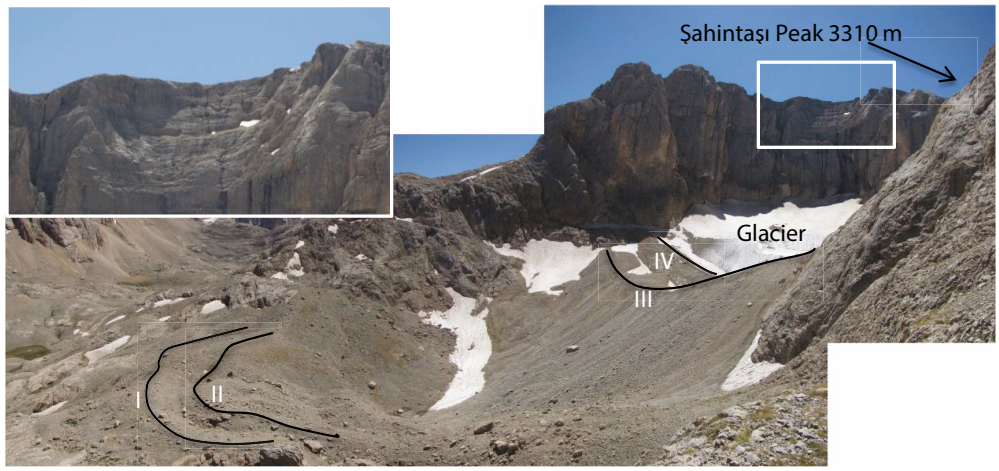

Figure 10. Şahintaşı Glacier and recessional and actual moraines (02.08.2013).

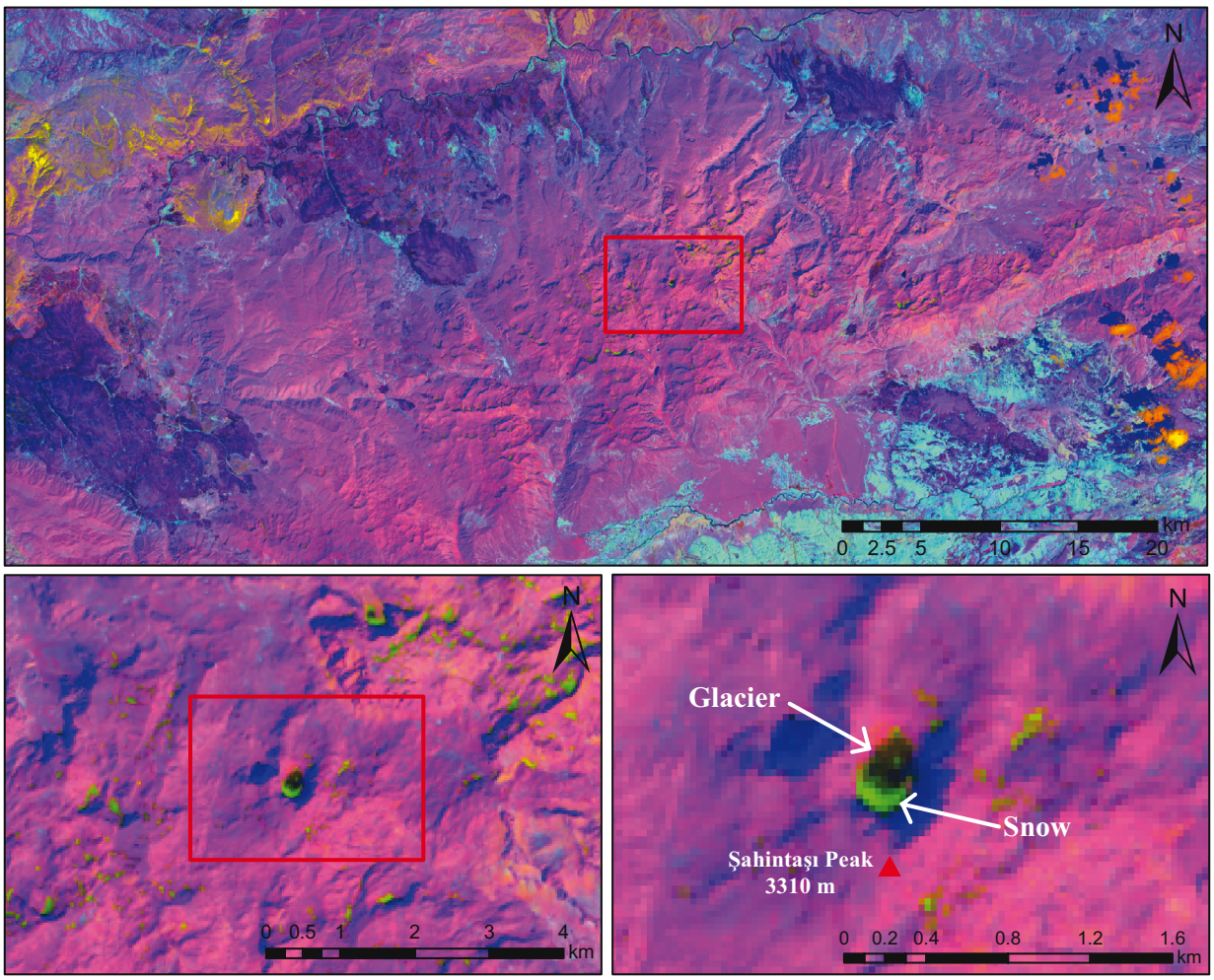

Figure 11. LANDSAT 8 L1T image (14 August 2013) enhanced by principal component analysis (black and light green colors reflect glaciers and snow, respectively).

Figure 12. The cirque Şahintaşı Glacier and paleokarstic depressions on the glacial valley extending to the north (02.08.2013).

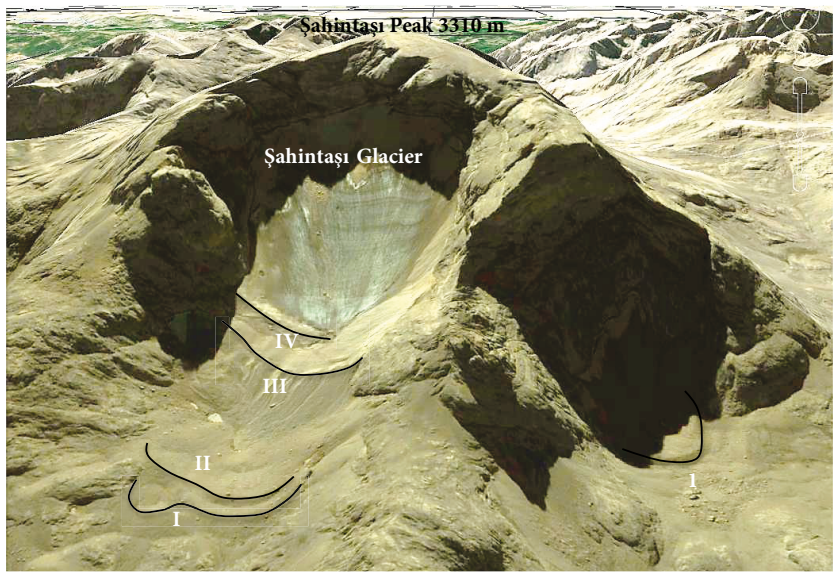

Figure 13. Google Earth image of Şahintaşı Glacier (view from north).

dating methods and to obtain precise information about the volume of the glaciers using geophysical methods.

Acknowledgments

We would like to express our deepest gratitude to Prof Dr Hüseyin Turoğlu (İstanbul University, Turkey), Prof Dr Murat Türkeş (Middle East Technical University, Turkey) and Asst. Prof Dr Faise Sarış (Çanakkale Onsekiz Mart University, Turkey) for their evaluations and contributions to the article. We are most grateful to Joseph S Oliphant and Peter Orte, as the copy editor of this study, for his meticulous proofreading and efforts to edit the paper. We also appreciate the helpful and constructive comments by PD Dr Naki Akçar (University of Bern, Switzerland), Assoc Prof M Akif Sarıkaya (İstanbul Technical University, Turkey), and an anonymous reviewer.

References

Akçar N, Schlüchter C (2005) Paleoglaciations in Anatolia: a schematic review and first results. Eiszeitalter und Gegenwart 55: 102–121.

Akçar N, Yavuz V, Ivy-Ochs S, Kubik PW, Vardar M, Schlüchter C (2008). A case for a downwasting mountain glacier during Termination I, Verçenik Valley, northeastern Turkey. J Quaternary Sci 23: 273–285.

Atalay İ (1987). Türkiye jeomorfolojine giriş. İzmir, Turkey: Ege University (in Turkish).

Bayrakdar C (2012). Akdağ Kütlesi'nde (*Batı Toroslar*) karstlaşma-buzul ilişkisinin jeomorfolojik analizi. PhD, İstanbul University, İstanbul, Turkey (in Turkish).

Bilgin T (1969). Gavur Dağı kütlesinde glasyal ve periglasiyal topografya şekilleri. İstanbul, Turkey: İÜ Coğrafya Enstitüsü (in Turkish).

Bilgin T (1972). Munzur Dağlarının doğu kısmının glasyal ve periglasyal morfoloji. İstanbul, Turkey: İÜ Coğrafya Enstitüsü (in Turkish).

Çılğın Z (2013). The influence of glacıatıon on the geomorphology of Ovacık Plain (Tunceli) and southwest catchment of Munzur Mountaın. Kilis 7 Aralık Üniversitesi Sosyal Bilimler Dergisi 6: 103–121 (in Turkish with English abstract).

Çılğın Z, Bayrakdar C, Oliphant JS (2014). An example of polygenetic geomorphologic development (karst-glacial-tectonics) on Munzur Mountains: Kepir Cave-Elbaba Spring karstic system. Int J Hum Sci 11: 89–104.

Çiner A (2003). Recent glaciers and late quaternary glacial deposits of Turkey. Geological Bulletin of Turkey 46 : 55–78.

Doğu AF, Somuncu M, Çiçek İ, Tunçel H, Gürgen G (1993). Kaçkar Dağında buzul şekilleri, yaylalar ve turizm. AÜ Türkiye Coğrafyası Dergisi 2: 157–184 (in Turkish).

Erinç S (1945). Doğu Karadeniz Dağlarında glasyal morfoloji araştırmaları. İstanbul, Turkey: İstanbul University (in Turkish).

Erinç S (1951). Glasiyal ve postglasiyal safhada Erciyes glasiyesi. İstanbul Üniversitesi Coğrafya Enstitüsü Dergisi 1: 82–90 (in Turkish).

Erinç S (1952). The present day glaciation in Turkey. In: 8th General Assembly and 17th International Congress of the International Geographical Union, Proceedings. Washington, DC, USA: International Geographical Union, pp. 326–330.

Erinç S (1953). Van'dan Cilo Dağlarına. İstanbul Üniversitesi Coğrafya Enstitüsü Dergisi 2: 84–106 (in Turkish).

Erinç S (1971). Jeomorfoloji II. İstanbul, Turkey: İstanbul Üniversitesi Coğrafya Enstitüsü (in Turkish).

Faust N (1989). "Image Enhancement." Volume 20, Supplement 5 of the Encyclopedia of Computer Science and Technology. New York, NY, USA: Marcel Dekker.

Gao J, Liu Y (2001). Applications of remote sensing, GIS and GPS in glaciology: a review. Pro Phy Geogr 25: 520–540.

Gürgen G, Yeşilyurt S (2012). Karçal Mountain glaciers (Artvin-Turkey). Coğrafi Bilimler Dergisi 10: 91–104 (in Turkish with English abstract).

Hall DK, Martinec J (1985). Remote Sensing of Ice and Snow. London, UK: Chapman and Hall.

Hambrey MJ (1994) Glacial Environments. London, UK: UCL Press.

Hubbard B, Glasser N (2005). Field Techniques in Glaciology and Geomorphology. Chichester, UK: John Wiley & Sons.

Iyigun C, Türkeş M, Batmaz İ, Yozgatligil C, Purutçuoğlu V, Koç EK, Öztürk MZ (2013). Clustering current climate regions of Turkey by using a multivariate statistical method. Theo App Clima 114: 95–106.

Jackson BB (1983). Multivariate Data Analysis: An Introduction. Irwin, IL, USA: Homewood.

Jensen JR (1996). Introductory Image Processing: A Remote Sensing Perspective. London, UK: Prentice Hall.

Klimchouk A, Bayari S, Nazik L, Törk K (2006). Glacial destruction of cave systems in high mountains, with a special reference to the Aladaglar Massif, Central Taurus, Turkey. Acta Carso 35: 111–121.

Konig M, Winther JG, Isaksson E (2001). Measuring snow and ice properties from satellite. Rev Geophys 39: 1–28.

Kurter A, Sungur K (1991). Glaciers of the Middle East and Africa - glaciers of Turkey. US Geological Survey Professional Paper 1386-G-l. Reston, VA, USA: USGS.

Lillesand TM, Kiefer RW (2004). Remote Sensing and Image Interpretation. New York, NY, USA: John Wiley.

Messerli B (1967). Die Eiszeitliche und die Gegenwartige Vergletscherung in Mittelmeerraum. Geographica Helvetica 22: 105–228 (in German).

Özgül N (1981). Munzur Dağlarının jeolojisi. Ankara, Turkey: MTA.

Paterson W (1994). The Physics of Glaciers. Oxford, UK: Pergamon Press.

Rees WG (2001). Physical Principles of Remote Sensing. 2nd ed. Cambridge, UK: Cambridge University Press.

Roy DP, Wulder MA, Loveland TR, Woodcock CE, Allen RG, Anderson MC, Helder D, Irons JR, Johnson DM, Kennedy R et al. (2014). LANDSAT-8: Science and product vision for terrestrial global change research. Remote Sens Environ 145: 154–172.

Sarikaya MA (2012). Recession of the ice cap on Mount Ağrı (Ararat), Turkey, from 1976 to 2011 and its climatic significance. J Asian Earth Sci 46: 190–194.

Sarıkaya M, Çiner A, Zreda M (2011). Quaternary glaciations of Turkey. In: Ehlers J, Gibbard P, Hughes P, editors. Quaternary Glaciations - Extent and Chronology. Oxford, UK: Jordan Hill, pp. 393–403.

Sarıkaya MA, Zreda M, Çiner A (2009). Glaciations and paleoclimate of Mount Erciyes, central Turkey, since the Last Glacial Maximum, inferred from ^{36}Cl cosmogenic dating and glacier modeling. Quaternary Sci Rev 28: 2326–2341.

Sarıkaya MA, Zreda M, Çiner A, Zweck C (2008). Cold and wet Last Glacial Maximum on Mount Sandıras, SW Turkey, inferred from cosmogenic dating and glacier modeling. Quaternary Sci Rev 27: 769–780.

Singh A, Harrison A (1985). Standardized principal components. Int J Remote Sens 6: 885–896.

Sugden DE, John BS (1976) Glaciers and Landscape: A Geomorphological Approach. London, UK: Edward Arnold.

Türkeş M (2010). Klimatoloji ve meteoroloji. 1st ed. İstanbul, Turkey: Kriter Yayınevi (in Turkish).

Türkeş M, Tatlı H (2011). Türkiye yağış bölgelerinin spektral kümeleme tekniğiyle belirlenmesi. In: Proceedings of the National Geographical Congress with International Participation, İstanbul, Turkey (CD-ROM).

Yeşilyurt S (2010). CBS ve uzaktan algılama yöntemleriyle munzur dağları glasyal jeomorfolojisinin analizi. Ankara, Turkey: Ankara Üniversitesi Sosyal Bilimler Enstitüsü Dönem Projesi (in Turkish).

Yeşilyurt S (2012). Late Quaternary glaciations of the Munzur Mountains, Eastern Anatolia, Turkey: an assessment using remote sensing and GIS techniques. In: XVIII INQUA Congress; 21–27 July 2011; Bern, Switzerland. Abstracts/ Quaternary International 279–280: 548.